LUND UNIVERSITY

Nanosecond image processing using stimulated photon echoes

Xu, E. Y; Kröll, Stefan; Huestis, D. L; Kachru, R; Kim, M. K

Link to publication

Total number of authors:
5

Nanosecond image processing using stimulated photon echoes

E. Y. Xu, S. Kröll, D. L. Huestis, and R. Kachru

Molecular Physics Laboratory, SRI International, Menlo Park, California 94025

M. K. Kim

Department of Physics and Astronomy, Wayne State University, Detroit, Michigan 48202

Processing of two-dimensional images on a nanosecond time scale is demonstrated using the stimulated photon echoes in a rare-earth-doped crystal (0.1 at. % Pr^{3+}:LaF_3). Two spatially encoded laser pulses (pictures) resonant with the $^3P_0$–$^3H_4$ transition of Pr^{3+} were stored by focusing the image pulses sequentially into the Pr^{3+}:LaF_3 crystal. The stored information is retrieved and processed by a third read pulse, generating the echo that is the spatial convolution or correlation of the input images. Application of this scheme to high-speed pattern recognition is discussed.

High-speed real-time processing of two-dimensional images has a variety of applications in which large numbers of images must be stored and analyzed, such as in robotic vision, satellite remote sensing, medical image analysis, artificial intelligence, and pattern recognition. Optical image processing is promising for two principal reasons: parallel processing capability and potentially ultrafast speed. Among the existing techniques for two-dimensional image processing are digital computer processing, Vander Lugt holography,[1] four-wave mixing in photorefractive materials,[2-4] and neural networks.[5,6] Improvements to the Vander Lugt approach, most notably the use of phase-only filters, have been suggested[2] and demonstrated.[4-8] However, these improvements do not overcome the speed limitation arising from the use of filters.

Several groups[2-4,9] have investigated the use of transient masks in nonlinear-optical materials. Pepper *et al.*[2] have suggested, and White and Yariv[3] and Odulov and Soskin[4] have demonstrated, a practical way to perform optical correlation and convolution between two images using degenerate four-wave mixing. Owing to the charge migration time, the process is slow at low laser fluences: approximately 100 msec in oxide crystals and 1 μsec in semiconductor materials. Nevertheless, they are important materials in long-term storage applications.

We report in this Letter the demonstration of two-dimensional image processing in a crystal on a nanosecond time scale using the backward stimulated photon echo technique.[10-21] The processing speed that we have demonstrated is 10^5 times faster than that obtained previously with oxide-type photorefractive materials. This is because the excitation of a resonant transition provides the forming of transient population grating in the crystals rather than inducing transportation of charges. The image processor in this experiment is the $^3P_0$–$^3H_4$ transition of Pr^{3+}:LaF_3. Spatially encoded laser pulses (pictures) are focused sequentially into the crystal at the transition wavelength of 477.8 nm. The stored information is re-

trieved by a read pulse into an echo image that carries spatial convolution and correlation of the input images.

Consider an assembly of ions with a center frequency ω_0. For simplicity, we assume that the laser electric fields of all excitation pulses are monochromatic and at a frequency ω_0. The coherent nature of the data pulse input into the sample at time $t_1 = 0$ (see Fig. 1) results in the electric dipole of the ion's acquiring the phase of the excitation electric field. Subsequent to the passage of the data pulse, the dipole oscillates at its own natural absorption frequency ω. The write pulse that passes through the sample at $t_2 = \tau$ either constructively or destructively interferes with the (first) data pulse, depending on whether the dipoles that were excited by the data pulse are in or out of
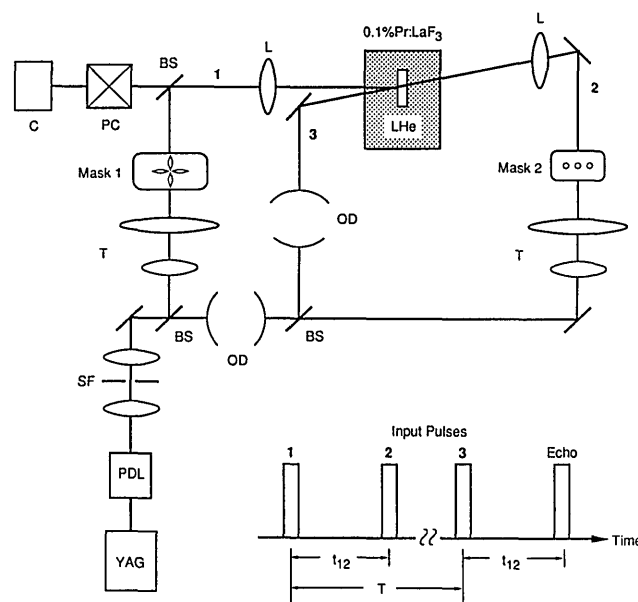

Fig. 1.   Schematic of the experimental apparatus for the optical image processor. OD, optical delay line; C, camera.

phase with the write pulse. Dipoles with absorption frequency $\omega_0 = \omega_0 + \Delta\omega$ are in (out of) phase with the write pulse if $\Delta\omega\tau$ is a (half) multiple of 2π. For these groups of ions the effect of the data and write pulse interfere constructively (destructively), yielding a strong (weak) excitation. The populations in the ground and excited states are therefore modulated after the passage of the write pulse as a function of $\Delta\omega$, with a frequency period of τ^{-1} that is the frequency Fourier transform of the temporal excitation pulse history. In general, if there are many data pulses, it can be shown that the population modulation pattern is proportional to the Fourier transform of the entire temporal sequence of data and write pulses. In principle, up to 10^{12} bits/cm^3 can be recorded in a sample such as Eu^{3+}:YAlO$_3$ (Ref. 19) or Pr^{3+}:YAG.[15] The information is stored as nonthermal population modulation in the ground-state hyperfine levels, which can last up to many hours in certain crystals.

When the sample is reexcited by the read pulse at a later time, spectral population modulation of the ground state is converted back to temporal modulation, consisting of a sequence of echo pulses that reproduce the original data pulse train.[10,18]

Now we consider convolution and correlation of images of the input pulse. Referring to Fig. 1, the sample crystal of thickness z_0 containing the impurity ion is resonantly excited at time t_i by three laser pulses of the form

$$\mathbf{E}_i(\mathbf{r}, t) = u_i(x, y)\exp[i(\mathbf{k}_i \cdot \mathbf{r} - \omega_0 t)] + \text{c.c.} \quad (i = 1, 2, 3),$$
(1)

where $u_i(\mathbf{r})$ is the slowly varying spatial envelope function. In Eq. (1), $i = 1, 2,$ and 3 refer to the data, write, and read image pulses, respectively. Pulse 1 propagates along the z axis, and pulses 2 and 3 counterpropagate to each other along an axis that has a small angle α with respect to the z axis. A pair of lenses of focal length F on each side of the sample focus these beams onto the sample at the common focal plane of the lenses. If we place an object mask at the outer focal plane of each of these beams so that $\mathbf{E}_i = u_i(x, y)$ at the mask, then this spatial profile is Fourier transformed by the lenses, so that the laser electric field at the focal plane of the input lens inside the crystal is $\tilde{u}_i(f_x, f_y)$. Here $\tilde{u}_i$ is the Fourier transform of u_i in the spatial frequencies $f_x = x_f/\lambda F$ and $f_y = y_f/\lambda F$, where λ is the laser wavelength. In the limit of a small pulse area, i.e., $\tilde{\theta}_i(f_x, f_y) < 1$, where $\tilde{\theta}_i(f_x, f_y) = \tilde{u}(f_x, f_y)\tau_p\mu/\hbar \ll 1$, with τ_p the temporal length of the ith pulse and μ the electric dipole moment of the optical transition, a macroscopic polarization P,

$$P \propto \tilde{u}_1 \otimes \tilde{u}_2 * \tilde{u}_3 \exp[i(-\mathbf{k}_1 + \mathbf{k}_2 + \mathbf{k}_3) \cdot \mathbf{r}],$$
(2)

is created at the echo time $t_e = t_3 + (t_2 - t_1)$.

Then it can be shown that the echo electric field at the outer focal plane is

$$E_e \propto u_3(-x, -y) * u_2(-x, -y) \otimes u_1(-x, -y)\exp(-ik_1 z),$$
(3)

where $\otimes$ and $*$ indicate spatial Fourier correlation and convolution, respectively.[1–4] If u_2 and u_3 are plane

waves (equivalent to point sources collimated by lenses), then the echo is a phase conjugate of pulse 1. Furthermore, if u_3 (u_2) is a plane wave, then the echo is the correlation of u_1 and u_2 (u_3). If u_1 is a plane wave, then the echo is a convolution of u_2 and u_3.

The experimental setup to demonstrate the image processing between a data image and the read or write image by the stimulated photon echo is shown in Fig. 1. A YAG-laser-pumped pulsed dye laser (PDL) with a 2-GHz linewidth is tuned at 477.8 nm for the $^3H_4$–$^3P_0$ transition of Pr^{3+}:LaF$_3$. A spatial filter (SF) is used to improve the spatial beam profile of the laser. Two beam splitters (BS) divide the laser beam into three parts, two of which are optically delayed by 80 and 90 nsec, respectively. Each laser pulse typically has an energy of 50 μJ and a cross-section area of 1 mm^2. Before going through the transmission object masks, the beams are expanded by telescopes (T) so that they illuminate the entire patterns uniformly. The dotted masks were made of thin aluminum plates with small holes. The letter pattern was cut on aluminum foil, which was then attached to a microscope slide. The first beam passes through the data mask and is focused by a 50-cm focal-length lens (L) into the crystal. The second beam, encoded with the write image, is focused by another 50-cm lens (L) and enters the crystal from the opposite direction. The lenses share a common focal plane. The plane-wave read beam counterpropagates with respect to the write beam. In another configuration, the read beam carried the spatial image while the write beam was a plane wave. The emitted echo image counterpropagates with respect to the data beam and is picked off by a beam splitter. A gated Pockels cell (PC) between crossed polarizers transmits the echo while blocking scattered light from the input pulses. The echo image was the sharpest at the same distance from the sample as the data image because the echo image is the phase conjugate of the data image. To perform the convolution correctly, the thickness of the crystal has to be within the good focal plane of the lenses, defined as the depth of focus of the lens, where the intensity distribution is a faithful Fourier transform of the original image. This thickness is given in Ref. 4 as $z_0 \ll \lambda F^2/(\pi d^2)$, where F is the focal length and d is the beam aperture diameter. In our case, z_0 is 1.5 mm, and the crystal was cut to less than 1 mm thick to avoid this length aberration.

Echo images were recorded with a camera using fast Polaroid film. Figure 2 shows the stimulated photon echo image processing result with five different experimental configurations. Figure 2(a) is an image reproduction with plane-wave inputs of write and read beams. Figure 2(b) is an image convolution case with one x and two dots yielding two x's. Figures 2(c) and 2(e) are correlation operations. When the data image rotates by 90° in Fig. 2(e), so does the echo image. The haze around the echo dots are the write pulse leakage through the Pockels cell. The dots in the data image are typically 5 mm apart. In some echo images the edges are blocked by the 1-cm Pockels cell aperture.

Efficient high-speed pattern recognition using Fourier transformations requires two developments: a
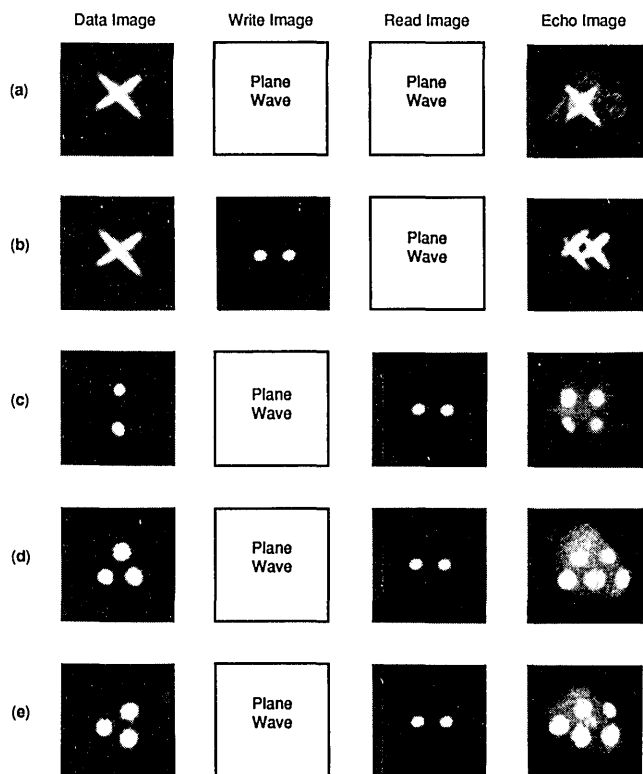
Fig. 2.   Photographs of input and output images.   (a) Image reproduction, (b) image convolution, and (c)–(e) image correlations.

fast image processor and identification of strategies for choosing the analysis images with which the unknown image should be convolved or correlated. The stimulated echo image processor will satisfy the first need. We can begin with the naive strategy of storing large numbers of reference images containing features that we hope to find or recognize in the test image to be analyzed. Thus, as an initial approach we could encode a set of data pulses with several reference matched filters (one filter in each pulse). The encoded data pulses are then written into the crystal with a uniform-intensity write pulse. The picture to be analyzed is then provided in the read pulse. The sequence of echoes (or output images) reveals the correlation between the picture to be analyzed and each of the previously stored reference images. Because the crystal is also an image memory device,[17,18] the images to be analyzed can be applied either immediately (the read pulse is temporally coincident with the write pulse) or after a short or extended delay (100 μsec to hours or potentially days). Furthermore, the reference images can be used to analyze a number of objects before the stored images need to be refreshed.

In conclusion, we have successfully demonstrated

spatial convolution and correlation of input images on nanosecond time scales. There is a potential of storing spatial information in the processor and accurately retrieving it after a long time delay (hours) as has been accomplished with $Eu^{3+}:YAlO_3$ (Ref. 19) and $Eu^{3+}:Y_2O_3$.[22] Combining the nanosecond processing capability that we have demonstrated with the ultrafast high-density storage potential, the stimulated echo technique has attractive potential applications in two-dimensional image processing and pattern recognition. Although the image quality needs improvement, the results shown in Fig. 2 clearly demonstrate the ability of backward stimulated echoes to perform spatial correlation on a nanosecond time scale.

References

1. A. B. Vander Lugt, IEEE Trans. Inf. Theory **IT-10**, 2 (1964).
2. D. M. Pepper, J. Au Yeung, D. Fekete, and A. Yariv, Opt. Lett. **3**, (1978).
3. J. O. White and A. Yariv, Appl. Phys. Lett. **1**, 37 (1980).
4. S. G. Odulov and M. S. Soskin, Sov. Phys. Dokl. **25**, 5 (1980).
5. E. G. Paek and D. Psaltis, Opt. Eng. **26**, 428 (1987).
6. L.-S. Lee, H. M. Stoll, and M. C. Tackitt, Opt. Lett. **14**, 162 (1989).
7. J. L. Horner and J. R. Leger, Appl. Opt. **24**, 609 (1985); J. L. Horner and H. O. Bartlett, Appl. Opt. **24**, 2889 (1985).
8. D. Psaltis, E. G. Paek, and S. S. Verkatsh, Opt. Eng. **23**, 698 (1984).
9. S. H. Lee, Opt. Eng. **13**, 196 (1974).
10. T. W. Mossberg, Opt. Lett. **7**, 77 (1982).
11. N. W. Carlson, L. J. Rothberg, A. G. Yodh, W. R. Babbitt, and T. W. Mossberg, Opt. Lett. **8**, 483 (1983).
12. N. W. Carlson, W. R. Babbitt, and T. W. Mossberg, Opt. Lett. **8**, 623 (1983).
13. N. W. Carlson, W. R. Babbitt, Y. S. Bai, and T. W. Mossberg, J. Opt. Soc. Am. B **2**, 908 (1985).
14. Y. S. Bai, W. R. Babbitt, and T. W. Mossberg, Opt. Lett. **11**, 724 (1986).
15. W. R. Babbitt and T. W. Mossberg, Opt. Commun. **65**, 185 (1988).
16. P. Saari, R. Kaarli, and A. Rebane, J. Opt. Soc. Am. B **3**, 527 (1986).
17. M. K. Kim and R. Kachru, J. Opt. Soc. Am. B **4**, 305 (1987).
18. M. K. Kim and R. Kachru, Opt. Lett. **12**, 593 (1987).
19. M. K. Kim and R. Kachru, Opt. Lett. **14**, 423 (1989).
20. Y. S. Bai, W. R. Babbitt, N. W. Carlson, and T. W. Mossberg, Appl. Phys. Lett. **45**, 1714 (1984).
21. M. K. Kim and R. Kachru, Appl. Opt. **28**, 2186 (1989).
22. W. R. Babbitt, A. Lezama, and T. W. Mossberg, Phys. Rev. B **39**, 1987 (1989).